Mössbauer Effect and its Application to Material Research†

Toshio ENJYO* and Saburo NASU**

Abstract

Principles of the Mössbauer effect and the hyperfine interaction parameters evaluated from the Mössbauer spectra are summarized and discussed in view of material research. Precipitation study of iron in aluminum and the estimation of the ferrite content in stainless steel weld and casting, both of which were reported already, are presented again as typical applications of the Fe^{57} Mössbauer spectrometry.

1. Introduction

When the energy states of the nucleus are defined as a ground state and excited states only by the decay of gamma ray radiation, there is a possibility to observe the resonant absorption by the incident photon whose energy exactly equal to the energy separation of the nuclear energy levels. However the momentum conservation requires the recoil energy E_R for the emitted nucleus like the recoilling cannon. Absorbing nucleus also require the extra energy of E_R and the total $2E_R$ excess energy needs for the resonant absorption by the nuclear gamma ray radiation. Actually it is extremely difficult for the free nucleus to observe the resonant absorption by the nuclear gamma ray radiation.

Rudolf Mössbauer successfully discovered the recoilless resonance absorption of gamma radiation in Ir^{191} nucleus and got the Nobel Prize in 1961 for his discovery[1~4]. We can easily understand his ideas to get this brilliant discovery as follows. When the recoil energy E_R by the gamma radiation from the nuclei embedded in the solid lattiee is larger than the binding energy of the atoms in solid lattice, the atom is kick out from the lattice points. When the recoil energy, on the other hand, is smaller than the binding energy and still smaller than the excitation energy for the quantum states of the lattice, the gamma radiation has a large probability to find the resonance absorption by the nuclei. This recoilless nuclear resonancet absorption of gamma radiation is called as a Mössbauer effect.

Mössbauer effect is originally nuclear events belong to one branch of the nuclear gamma ray spectroscopy and the energy of the gamma radiation directly depends on the nuclear structure and the hyperfine interactions between the nuclear and the surrounding electric states. Nuclear parameters are generally independent to the electric and atomic states in solid. Then the Mössbauer effect measurements can offer the electric and atomic parameters in hyperfine interections from our knowledge on the nuclear parameters[5~8]

Experimentally the resonant absorption and the acurate energy difference can be observed in the couple of the emitter nucleus and the absorber nucleus in which the gamma ray energy of one side nucleus is modulated by the externally supplied Doppler effect. There are many isotopes in which the Mössbauer effects were observed and are shown in a periodic table as **Table 1.** From the hyperfine interaction observed in these isotopes, the Mössbauer effect offers the broad contribution to the many fields of the natural science[9~16].

In this report, the parameters derived from Fe^{57} Mössbauer effects are summarized in Section 3 and two applications for material science are presented in Section 4.

2. Instrumentation

The Mössbauer effect measurements can be performed by same instruments as used in nuclear gamma ray spectrametry as previously mentioned. Many commercial spectrometer for Mössbauer effect measurements are used to the applied research in recent years.

Instruments consist of three parts. One part is a gamma ray source and absorber. Both are available for the specimen. The second part is a gamma ray modulator. Electro-magnetic transducer and the mechanical modulation system are used for the creation of the Doppler velocity for the gamma radiation. Third part is a storing and counting system for the incident or scattered gamma ray as a function of the Doppler velodity. Proportional counter and scientla-

† Received on July 25, 1974
* Professor
** Research Instructor

Table 1. Mössbauer periodic table. (Ref. 14)

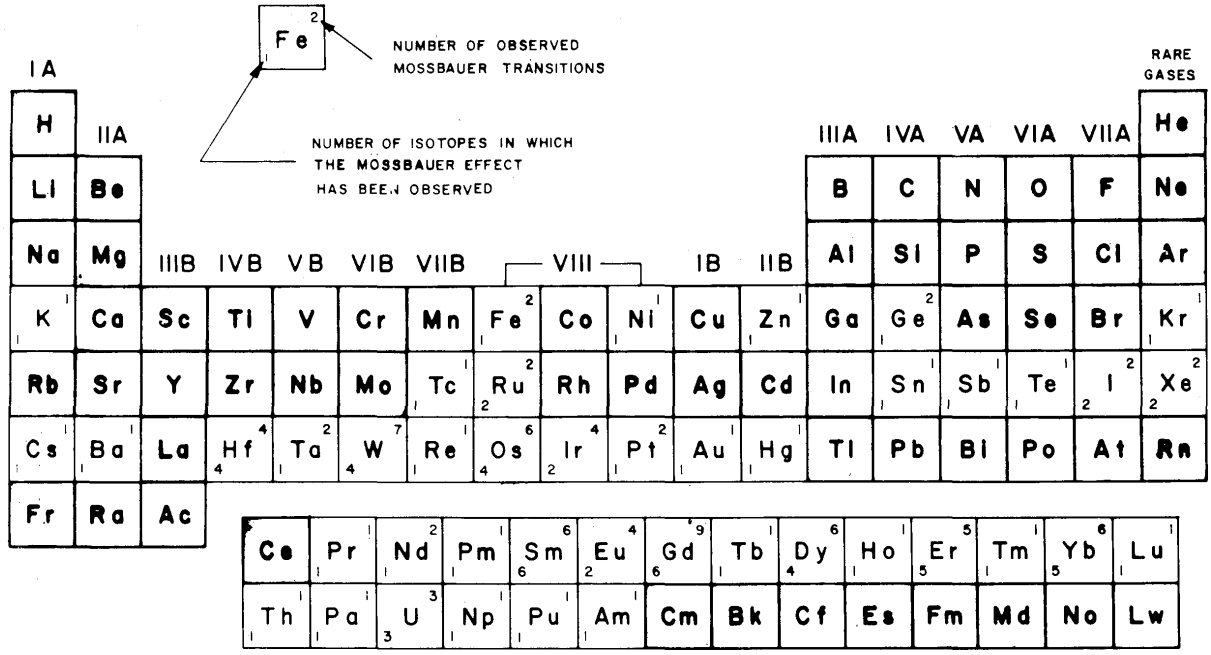

tion counter are used as a gamma ray detector. Surrounding apparatus for storing system consist of pulse height analyser, variable amplifier, high voltage supply and so on. **Figure 1 (a)** shows the principle arrangements for the observation both of resonance and scattering. Figure 1 **(b)** shows the typical spectra obtained from the single line source and the absorber. Scattering spectrum was obtained by the re-emitting

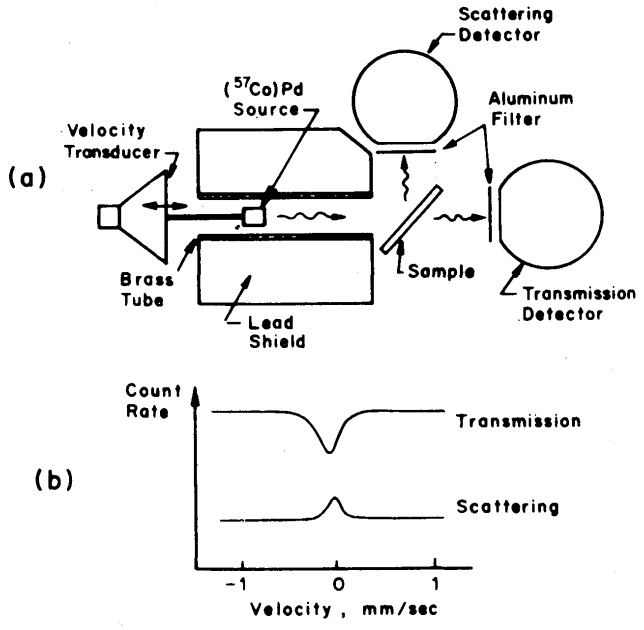

Fig. 1. (a) Experimental arrangement for observing the Mössbauer effect by scattering or transmission for a thin sample. The scattering experiment can also be performed on a thick sample.
(b) Schematic comparison of spectra obtained by transmission and scattering geometry from Swartzendruber et al. (Ref. 17).

of the gamma ray (and/or more low energy electron and X-ray) followed by the subsequent decay of the resonant nucleus. Scattering technique using conversion electron is very important for the surface study because the large attenuation and absorption of the electron energy occured near the surface and only selective nucleus are available for the counting in the case of the scattering geometry[18),19)]. And for the quite thick bulk materials the scattering geometry is only possible to utilize the Mössbauer effect[17)].

3. Mössbauer Parameters

Mössbauer parameters include principally nuclear factors as previously mentioned. Difference in the nuclear charge radius $\Delta R/R$, nuclear magnetic dipole moments μ, nuclear quadrupole moments Q and spins I, nuclear lifetime τ and internal convension coefficient α are directry concerned to the Mössbauer effects. However above nuclear parameters may be independent to the temperature, pressure and the other properties of solid. Our attension must pay for the electric and the solid state factors obtained from hyperfine interactions between electrons and nucleus.

3.1 Recoilless resonant fraction

Probability for a transition in which the nucleus decays from the excited states N_i to the ground state N_f, while simultaneously the lattice goes from its initial state L_i to its final state L_f is

$$W(N_i \rightarrow N_f,\ L_i \rightarrow L_f) = \text{const} \cdot |\langle f|\, H_{int.}\, |i\rangle|^2$$

where $<i|$ and $<f|$ denote the initial and final state of the entire system, including the lattice and H_{int} is the interaction Hamiltonian responsible for this decay. Because of the independence of the nuclear factors, the explicit form of the transition matrix element is given by

$$<f|H_{int.}|i>=<L_f|e^{ikx}|L_i>\cdot<N>$$

Here the nuclear matrix element $<N>$ depends only on nuclear properties, $k=p/\hbar$ is the wavevector of the emitted gamma ray, and X is the coordinate vector of the center of momentum of the decaying nucleus. $<L_f|\exp(ik\cdot X)|L_i>$ is the matrix element for transfer of a momentum $\hbar k$ to the lattice through the atom of the decaying nucleus with the lattice going from the state L_i to L_f. The calculation of the fraction f of gamma rays emitted without the energy loss to the lattice ($L_i \rightarrow L_i$) gives

$$f=|<L_i|\exp(ik\cdot X)|L_i>|^2 .$$

This equation has been the starting point for the most calculation of the recoilless resonant fraction f of gamma rays. Calculation were performed for the Einstein and Deye solid[5~9] and are given by

$$f=\exp\left(-\frac{R}{\hbar\omega_E}\right) \qquad \text{for Einstein solid.}$$

$$f=\exp\left[-\frac{6R}{k\theta_D}\left\{\frac{1}{4}+\left(\frac{T}{\theta_D}\right)^2\int_0^{\theta_D/T}\frac{x\,dx}{e^x-1}\right\}\right]$$

for Debye solid.

where R is the recoil energy. From f measurement, we can discuss about the lattice dynamical properties of solid[20), 21)].

3.2 Isomer shift (Electric monopolar interaction)

Nucleus has a charge radius and change slightly its energy state by the electrostatic interaction with the electron charge at the nucleus. If the charge radius of the excited state and ground state of the nuclei differ each other, we can observe the energy difference as a isomer shift value. Isomer shift in velocity unit is given by

$$\delta E=\frac{2}{5}\pi Z\cdot e^2\cdot|\psi(0)|^2\,[R_{ex.}^2-R_{gd.}^2],$$

where R_{ex} and R_{gd} indicate the charge radius for the excited and ground states. Experimentally isomer shift is given by the difference of the electron charge density between source and absorber material; that is

$$\text{I. S.}=\frac{2}{5}\pi Z\cdot e^2\,[\,|\psi_s(0)|^2-|\psi_a(0)|^2\,]\cdot[R_{ex.}^2-R_{gd.}^2].$$

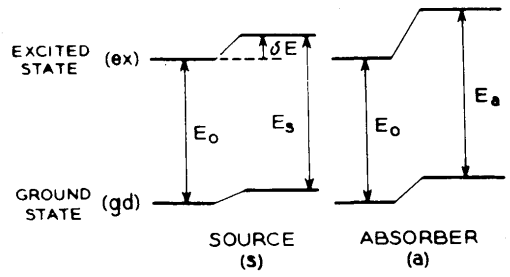

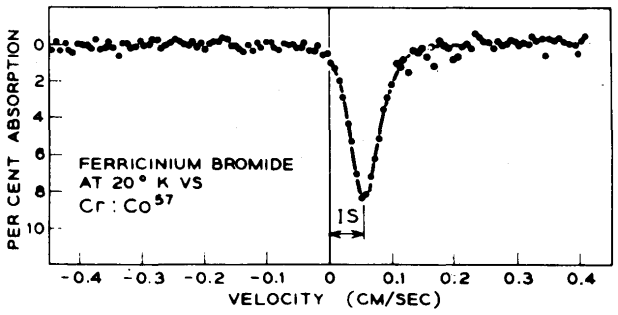

Fig. 2. Isomer shift. The effect of the electric monopole interaction on the nuclear levels and the resultant Mössbauer spectrum from Wertheim (Ref. 6), and Wertheim and Herber (Ref. 38).

Figure 2 shows the nuclear energy levels affected by the electrostatic interaction with the electric charge and also show the typical Mössbauer spectrum indicating the isomer shift of ionic state of the Fe^{57} atoms. Above equation clearly suggests that the difference of the s electron charge density at the resonant nuclei between the source material and absorber material can be discussed by the observed isomer shift values[22)]. For Fe^{57} and Sn^{119} Mössbauer effects, many standard isomer shift values are presented by several investigators[12~15)] and summarized in **Table 2** and **3.** A systematically variations of the Fe^{57} isomer shift in metals are shown in **Fig. 3**[6)]. For metals and alloys the quantitative discussion about the Fe^{57} isomer shift value are not completed, however Walker et al.[23)] calculated the isomer shift values using the total values for the $|\psi(0)|^2$ taking account for the shielding effects of the 3d electrons. From this relations, we can discuss about the electric states of the Fe^{57} atomic in ionic iron compounds. **Figure 4** shows the relationship between the isomer shift value and the electronic configurations for Fe atoms. Divalent iron and trivalent iron clearly indicate the specific isomer shift values and the degree of the covalency also can be discussed from this figure.

Discussion about one more physical parameter concerning the center shift observed in spectrum is not avoidable. This is the second order Doppler shift arising from the relativistic effect by the mass change after the nuclear decay accompanied large energy radiation[24)]. Second order Doppler shift is described

Table 2. Isomer shift scale for Fe^{57} (14.4 keV) in reference materials. (Ref. 14) Source and absorber at room temperature.
SNP=sodium nitprusside [$Na_2(CN)_5NO \cdot 2H_2O$]
SS =stainless steel
PFC=potassium ferrocyanide [$K_4(CN)_6 \cdot 3H_2O$]

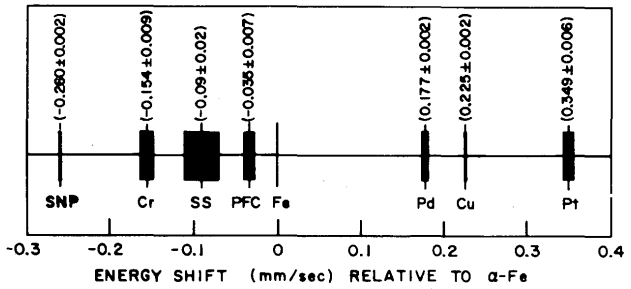

Table 3. Isomer shift scale for Sn^{119} source and reference materials. (Ref. 14) Source and aborber at room temperature except α-Sn which is at liquid nitrogen temperature and Mg_2Sn is given for both liquid nitrogen and room temperatures.
DMTF demethy tin difluoride [Me_2SnF_2]

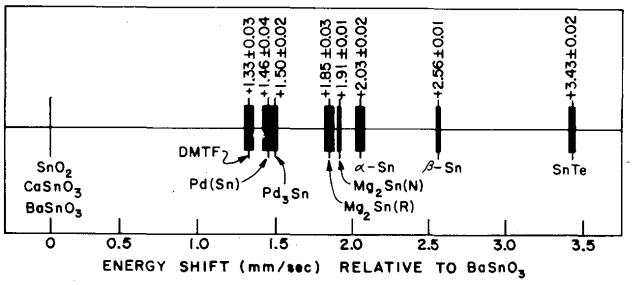

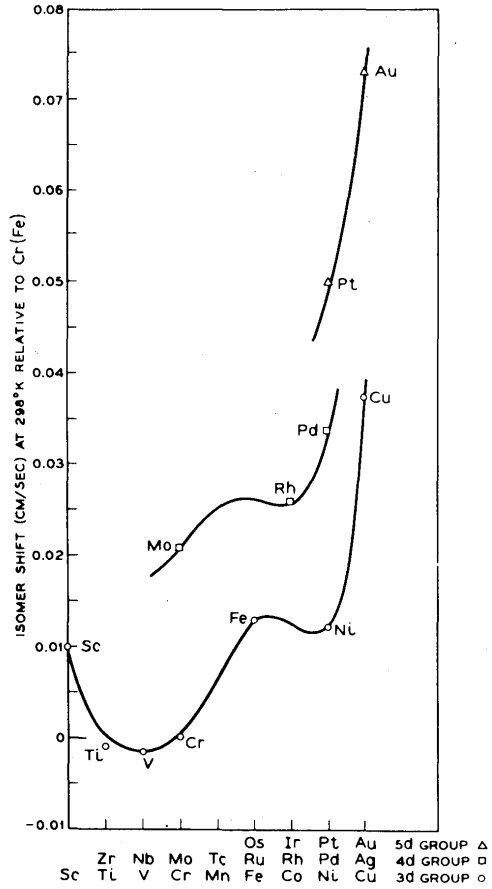

Fig. 3. Isomer shift of Fe^{57} in 3d, 4d and 5d group metals from Wertheim (Ref. 6).

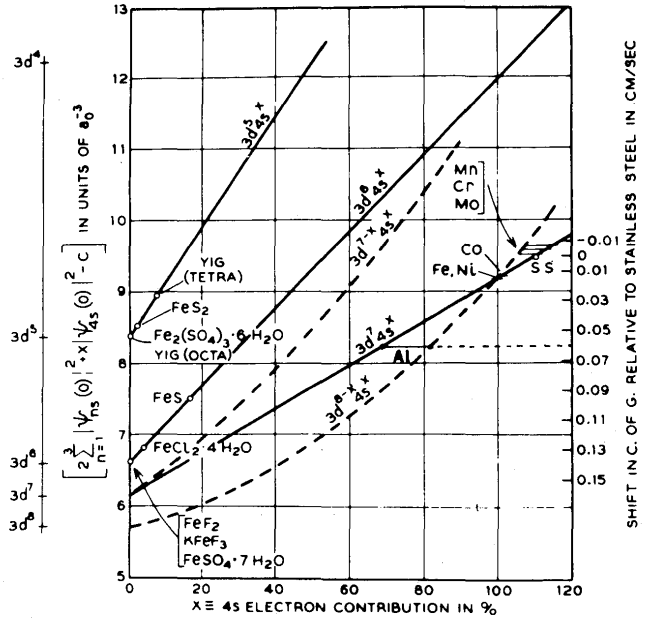

Fig. 4. The isomer shift of Fe^{57} as a function of 3d and 4s electron charge density from Walker at al., (Ref. 22)

by the mean-square velocity of the resonant nucleus and given in velocity unit by

$$\text{2nd order Doppler shift} = \langle V^2 \rangle / 2c$$

where c is the speed of light. Lattice dynamical properties including the zero point kinetic energy can be discussed by the above mean-square velocity of the resonant nuclei[25]

3.3 Nuclear quadrupole interaction

The discussion about the isomer shift was concerned with the effect of the electrostatic interaction between nuclear and electric charge at the nucleus. This effect was derived asuming the nucleus to be spherical and the charge density to be uniform. These conditions, however, are frequently destroyed and in fact higher order terms in the multipole expansion of the electrostatic interaction must be considered. These terms do not shift the nuclear levels but split them. They lift all or part of their $(2I+1)$ fold degenercy in which I is the nuclear spin quantum number.

The second term of the interaction of a nucleus with its surrounding electronic charge is the quadrupole interaction. This is the interaction of the nuclear quadrupole moment, Q, with the gradient of the electric field due to other charges in the crystal. The nuclear quadrupole moment reflects the deviation of the nucleus from spherical symmetry and given by

$$Q = \frac{1}{e} \int (3Z^2 - r^2) \cdot \rho(x, y, z) d\tau$$

where ρ denotes the charge density distribution within

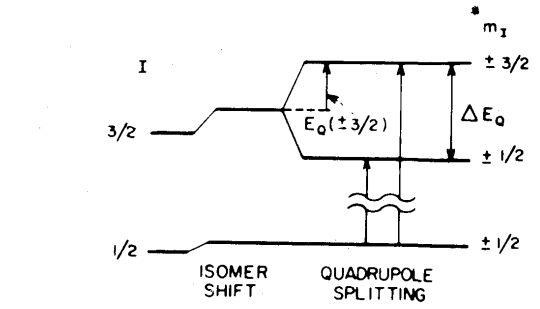

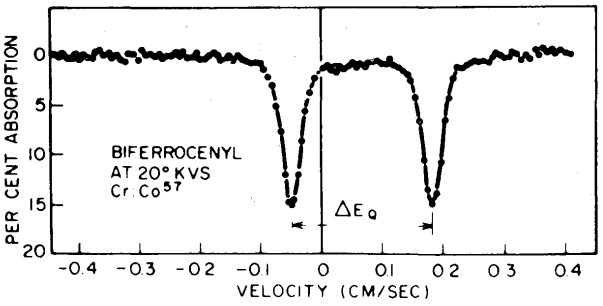

Fig. 5. Quadrupole splitting in Fe^{57} from Wertheim (Ref. 6) and Wertheim and Herber (Ref. 22).

the nucleus.

Interaction Hamiltonian between nuclear quadrupole moment, Q, and the electric field gradient is expressed by

$$H=\frac{eqQ}{4I(2I-1)}\left[3I_z^2-I(I+1)+\frac{\eta}{2}(I_+^2+I_-^2)\right]$$

where q is distant charge and I_+ and I_- are rasing and lowering operators. η is the asymmetry parameter and defined by

$$\eta=(V_{xx}-V_{yy})/V_{zz}$$

Energy eigenvalues are

$$E_Q=\frac{eqQ}{4I(2I-1)}\left[3\,m_I^2-I(I+1)\right]\cdot\left(1+\frac{\eta^2}{3}\right)^{\frac{1}{2}}$$

$$m_I \quad m_I=-I, -I+1, \ldots..I$$

Figure 5 shows the energy levels splitted by the pure quadrupole interaction and the resultant typical Mössbauer spectrum. From the quadrupole splitting in the Mössbauer spectrum, the informations about q and V_{zz} can be discussed. Microscopic investigations about the Fe electronic states using the above information are progress in coordination chemistry. For non S state ions, such as Fe^{2+}, the principal source of q, namely q_{val}, comes from integrating over the valence electrons on the Mössbauer ion itself, plus a secondary contribution q_{lat} from the rest of the crystal. Therefore total value of q is expressed by

$$q=(1-R)\cdot q_{val.}+(1-\gamma_\infty)\cdot q_{lat.},$$

where Sterheimer factors R and γ_∞ denotes the fraction of each electric field gradient source arising from deformed closed subshells in the Mössbauer atoms. For S state ion, such as Fe^{3+} the term of $(1-R)q_{val.}$ always vanishes.

However for metals and alloys the estimation of the q (effective) and V_{zz} is quite complicated because of the non uniform screening by the conduction electrons. Generally speaking the quadrupole interactions in metals and alloys are not large by the screening of the conduction electron in order to cancel the lattice contributions of the electric field gradient[26]. Even for the amorphous metallic material which shows the completely disordered atomic arrangements the magnitude of the quadrupole splitting was estimated to be smaller one comparing with that of the non-cubic iron ions in Fe compounds[27]

3.4 Magnetic hyperfine interaction

The interaction of the nuclear magnetic dipole moment μ with the magnetic field **H** due to the atom's own electrons is the most important term in hyperfine interactions.

The interaction Hamiltonian

$$H=-\mu\cdot\mathbf{H}=-g\cdot\mu\cdot\mathbf{I}\cdot\mathbf{H}$$

and the energy eigenvalues are

$$E_m=-g\cdot\mu\cdot H\cdot m_I$$
$$m_I=I, I-1, \ldots., -I.$$

Figure 6 shows the magnetic hyperfine splitting of the ground and excited state of Fe^{57}. The six allowed $\Delta m=0, \pm1$ transitions are indicated. Typical 6 line spectrum also shown in Fig. 6.

The magnetic hyperfine field from a single electron is

$$\mathbf{H}=-2\mu_B\left[\frac{8}{3}\pi\cdot|\psi(0)|^2\cdot\mathbf{s}+\left(\frac{1}{r^3}\right)+\left(\frac{3\mathbf{r}(\mathbf{s}\cdot\mathbf{r})-\mathbf{r}^2\cdot\mathbf{s}}{r^5}\right)\right]$$

The first term is the Fermi contact interaction and is only operable for s electrons. This term is observed as quite large field in a magnetic atom such as Fe or one of its ions. In such a case the magnetic 3d electrons polarized the inner s electrons via the exchange interaction that exists between electrons of like spin. Such a field is negative, that is, it is opposite to an externally applied field. The second term is due to the orbital contribution. It is small in many crystals because of quenching of the orbital angular momentum.

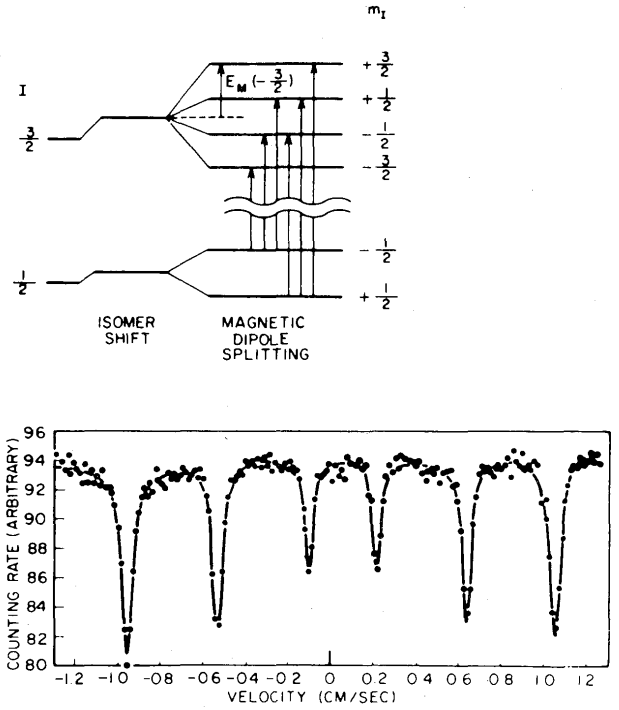

Fig. 6. Magnetic hyperfine splitting of the ground and first excited state of Fe^{57}. The Mössbauer spectrum obtained for FeF_3 at 4 K after Wertheim (Ref. 6).

The third term represents the dipole field due to the electron spin. These two terms are generally smaller than the contact term. Contact term depends on the number of the unparied 3d electrons as previously mentions. **Figure 7** shows the Slater-Pauling curve described by the Fe^{57} hyperfine field in alloys. This result clearly indicates the proportionality between the magnitude of the Fe^{57} hyperfine field and the saturation magnetization values. Detailed discussions about the magnetic hyperfine interaction and its application are presented already[28), 29)].

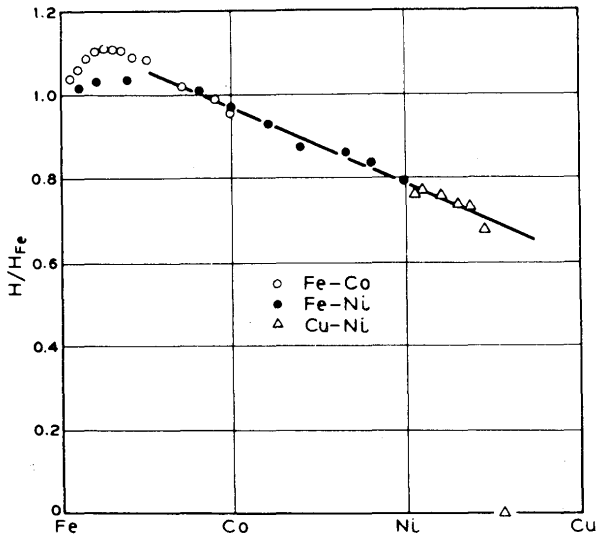

Fig. 7. Magnetic hyperfine field of Fe^{57} in various alloys plotted as a function of electron concentration after Wertheim (Ref. 6) and data from Boyle and Hall (Ref. 29).

The reason why the Mössbauer effect can offer so many fruitful results is surely the fact of successful observation of this hyperfine magnetic field. From this magnitude and sign of the hyperfine field, we can discuss about the magnetic properties to material and also recently we can use it as a diagnostic device for the better undestanding about the material condition[30), 31)]. For example the alloy composition was deduced from the magnitude of the Fe^{57} hyperfine field[17)].

4. Applications of the Fe^{57} Mössbauer Effect

4.1 Precipitation of Fe in aluminum

Age-hardenable alloys have been the subject of intensive theoretical and experimental studies in the field of physical metallurgy since an old time[32)]. A considerable body of the research works in the age-hardenable alloys are devoted to the study of thermodynamics and kinetics of the precipitation. There have been developed in progress of research techniques for the study of precipitation in alloys. Many fruitful results from precipitation phenomena have been obtaining using the X-ray diffraction techniques, thin foil electron microscopic observations and the electrical resistivity measurements[32)], however more accurate and microscopic investigations, i. e. the direct measurements of the electronic and vibrational local states of solute atoms and in precipitated particles, cannot be found in those research works. Direct observation of the ultra fine precipitated particles does not be possible by the usual technique and also it is very difficult even to determine the solid solubility of the solute atoms in a few alloy systems such as Al-Fe alloys containing small amounts of iron.

However, more microscopic investigations can be made possible by the analysis of the Mössbauer spectrum resulted from the hyperfine interactions between the nucleus of the solute atoms and their outer electrons[11), 33)]. Furthermore, the Mössbauer effects of the solute atom are directly indicated as a atomic situation after the diffusive motion of the solute atom and show the properties of the precipitated second phase which was formed by the Mössbauer active nuclei.

Small amount of the iron impurities are usually contained in a aluminum ingots and have played considerable important parts for the properties of commercial aluminum and its alloys[34)]. Fe^{57} Mössbauer spectrum of the Al-Fe alloys containing small amounts of iron can be separated into two parts; i. e. one arising from the solute iron atoms isolated in aluminum matrix and the other from the precipitated second phase.

Al-0.01 at. %Fe^{57} alloy was prepared by melting

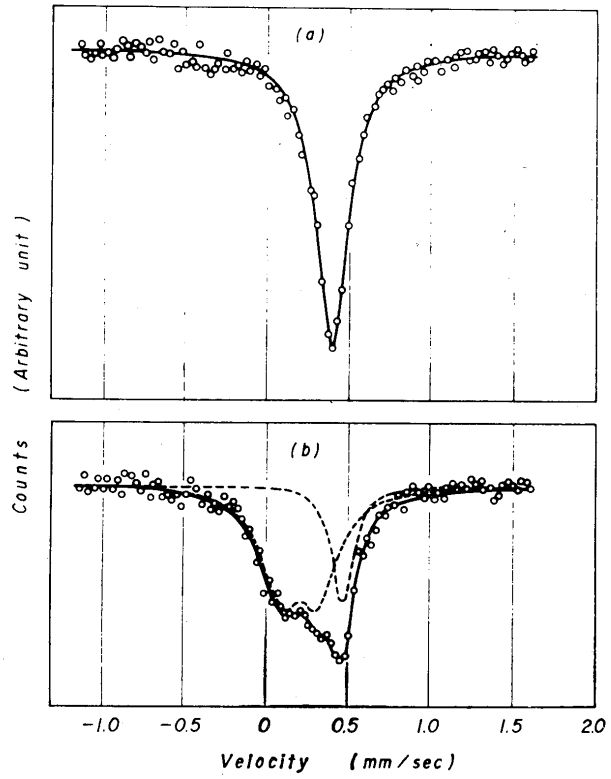

Fig. 8. Fe^{57} Mössbauer spectra obtained from a Al-0.01 at.%Fe alloy. (a) quenched specimen and (b) annealed specimen for 30 minutes at 450°C after cold rolling. Co^{57} in copper is used as a gamma ray source. Velocity indicates the relative to b.c.c. Fe at room temperature. (Ref. 36)

from 99.999 %Al ingot and the metallic Fe^{57} powders (ORNL stable isotopes, Fe^{57} 90 % up). This ingot was homogenized for 1 day at 643°C after cold rolling of 50 % reduction in thickness. The grain size was estimated to be about 2 mm and does not change its value during subsequent heat treatments. A square plate of the alloy specimen was cut from the ingot. Mössbauer effect measurements were performed by the transmission geometry. Thickness of the specimen was 0.5 mm which was selected for the good condition of the 14.4 keV gamma ray transmission intensity and the attenuation loss of the radiation.

Figure 8 shows the two Mössbauer spectra obtained from Al-0.01 at.%Fe^{57} alloy specimen. Upper spectrum (a) was measured by the specimen which was quenched into water immediately after the solution heat treatment at 650°C. Complete single line indicates the Fe^{57} atoms isolated in alloy matrix. That is, there is no quadrupole interaction and the cubic symmetry exists around the resonant Fe^{57} nucleus. Isomer shift value was estimated to be 0.42 ± 0.02 mm/sec relative to b. c. c. Fe at room temperature. Lower spectrum (b) was measured by the specimen whose composition is same as that for the spectrum (a), but aging treatment for 30 minutes at 450°C was added after cold rolling. The spectrum shows the superposition of a single line and doublet. Least-square fits for the Lorentz functions are performed with the aid of the digital computer. Doublet indicates the Fe^{57} atoms in precipitated second phase Al_6Fe, because its isomer shift value and the magnitude of the quadrupole splitting are identical to those of the Al_6Fe spectrum[35]. Figure 8 clearly shows the effects of the heat treatment for Fe precipitation in aluminum matrix. Determination of the solid solubility and the kinetics of the precipitated reaction of Fe in aluminum were investigated by the analysis of the Mössbauer spectra[36), 37)] **Figure 9** shows the computer output for the Fe^{57} Mössbauer effect in aluminum and the quantitative analysis can be done by the areal ratio between single line and doublet.

4.2 Ferrite content of stainless steel welds and castings

Recently NBS group performed excellent and first time application of the Fe^{57} Mössbauer spectrometry to the welded material research[17)]. Here we should like to present again their ideas and experimental results.

The presence of some ferrite in the microstructure of predominantly austenitic iron-chromium-nickel alloys has a significant influence on the physical and

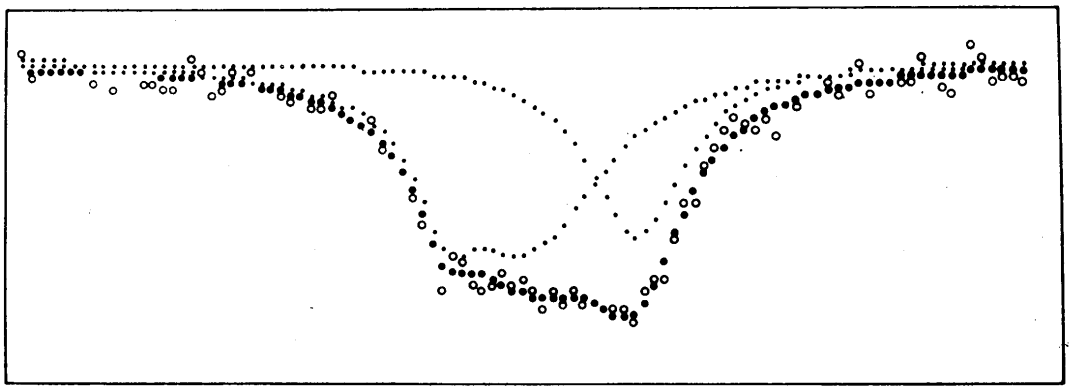

Fig. 9. Analyed Mössbauer spectrum which was plotted by computer. White circles indicate the experimental results and the dotted lines are analysed components and their superposition. (Ref. 36)

mechanical properties of the metal. Partially ferritic stainless weld metals are more resistant to fissuring or cracking during or immediately after welding of heavy sections. Improved welding characteristics, increased strength and substantially greater resistance to stress corrosion cracking are the chief attributes of the partially ferritic alloys in comparison to the wholly autenitic types. Full utilization of the benefits to be derived from such two phase materials have been hampered by difficulties in establishing their exact ferrite contents.

The Mössbauer effect scattering method measures the relative amounts of the austenite and ferrite phase on the basis of their magnetic properties in a way which is relatively independent of the shape, size and orientation of the ferrite particles. The method is nondestructive, requiring no special surface preparation and thus can be directly compared with standard magnetic measurements. Utilizing backscattered 14.4 keV gamma ray, they had obtained the first time Mössbauer spectra from a series of stainless steel welds and castings.

As mentioned in previous section, when different phases in a metal give well resolved Mössbauer spectra, the relative areas of the spectral patterns provide an indication of the amount of each phase present. The Mössbauer spectra for two distinct phases in an iron-chromium (45at.%Cr) alloy is shown in **Fig. 10 (b)** and **(c)** and compared with the spectrum

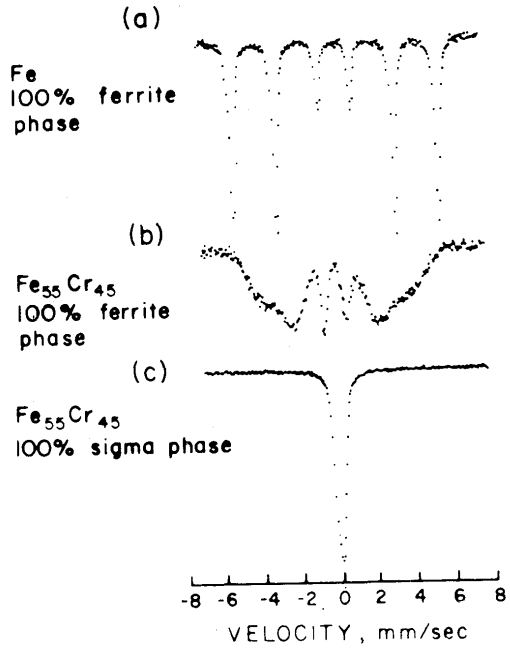

Fig. 10. Mössbauer absorption spectra for (a) a pure iron foil, (b) and Fe-45 at.%Cr alloy after annealing at 1000 C for one hour and quenching to room temperature to form single phase ferrite and (c) the same alloy after annealing at 775 C for 10 days to get the sigma phase from Swartzendruber er al., (Ref. 17).

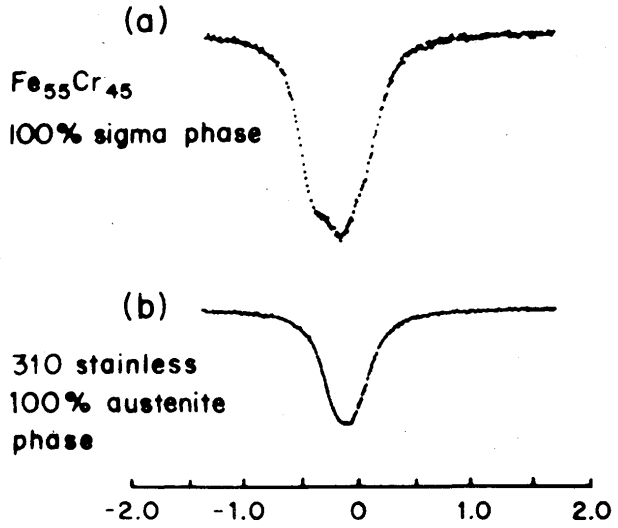

Fig. 11. Mössbauer absorption spectra from an Fe-Cr sigma phase and an austenitic stainless steel from Swartzendruber et al., (Ref. 17).

of pure iron in Fig. 10 **(a)**. The disordered (magnetic) and sigma (non-magnetic) phase in the Fe-Cr alloy clearly give two distinct spectral patterns and the composite spectrum from an alloy consisting of a mixture of these two phases could be resolved. **Figure 11** compares the spectrum from the same sigma phase with that from an austenitic stainless steel. Due to the expanded velocity scale, the structures of the phase spectrum is more readily apparent in Fig. 11 **(a)** than in Fig. 10 (c). Although these spectra are not as distinct as in the previous case, the efforts using the digital computer analysis might make possible to measure the fraction of sigma phase in a stainless steel. **Figure 12** shows the scattered Mössbauer spectra from weld sample 8B (0.047wt.%C, 0.31wt.%Si, 0.90wt.%Mn, 21.70wt.%Cr, 9.85wt.%Ni, 0.17wt.%Mo and 0.046 wt.%N), cast samples D2 (0.07wt.%C, 1.39wt.%Si, 0.79wt.%Mn, 20.17wt.%Cr, 9.55wt.%Ni, 2.40wt.%Mo and 0.06wt.%N) and K2 (0.30wt.%C, 0.91wt.%Si, 0.82wt.%Mn, 28.93wt.%Cr, 8.34wt.%Ni and 0.12wt. %N). The predominant peak in the center is from the austenite phase. The averaged magnetic hyperfine field estimated from the broad line contribution indicates the useful information about the ferrite compositions. Their Mössbauer results using the scattering technique have compared favorably with the assigned ferrite numbers for both the cast and weld materials for ferrite number less than about 20 %, but given significantly lower values of ferrite content in the 30～50 % ferrite range. The results from the magnetic hyperfine field measurements also provided confirmation that ferrite in as-weld metal responds more strongly magnetically than an equal amount of ferrite in casting.

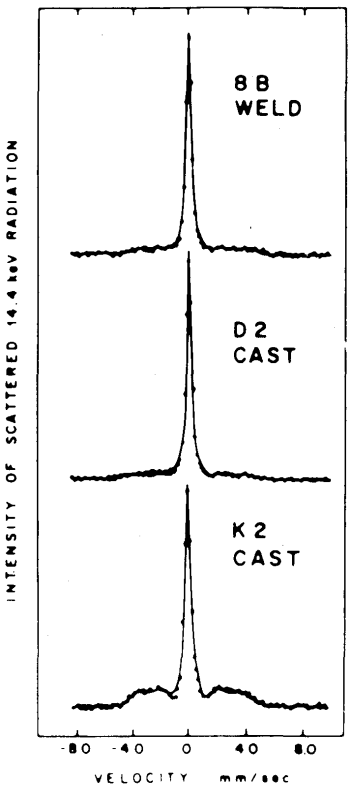

Fig. 12. Mössbauer scattering spectra from three weld and cast samples. The solid lines are a least square fit to a broad spectrum due to ferrite and to a narrow spectral line in the center due to austenite, from Swartzendruber et al., (Ref. 17).

5. Summary

The principle and fundamental parameters concerning the recoilless resonance of gamma radiation, so called, Mössbauer effect were summarized as terms of recoilless resonant fraction, isomer shift, nuclear quadrupole interaction, and magnetic hyperfine interaction.

Two typical research works were discussed as a example for the applicability of the Mössbauer effect to the material research. One is the precipitation study of iron in aluminum using the Fe^{57} Mössbauer spectra. The other is the recent work performed by the NBS group concerning the examination of ferrite content in stainless steel welds and castings using the scattered Fe^{57} Mössbauer spectra.

Acknowledgement

One of authors (S.N.) should like to thank Drs. L. J. Swartzendruber and L. H. Bennett for their sending of their preprint prior to their publication.

References

1) R. L. Mössbauer, Z. Physik, 151 (1958) 124.
2) R. L. Mössbauer, Z. Naturforsch, 14a (1959) 211.
3) R. L. Mössbauer, Naturwissenschaften, 45 (1958a) 538.
4) R. L. Mössbauer, Noble Lecture, December 11, 1961.
5) H. Frauenfelder, The Mössbauer Effect. (W. A. Benjamin, New York, 1964).
6) G. K. Wertheim, Mössbauer Effect: Principles and Applications. (Academic Press, New York, 1964).
7) H. Wegener, Der Mössbauer-Effekt und seine Anwendung in Physik und Chemie. (Bibliographisches Institut, Mannheim, 1968).
8) C. Janot, L'Effe Mössbauer et ses Applications, a la Physique du Solide et a la Métallurgie Physique. (Masson et C^{ie}, Paris, 1972).
9) L. May, Ed., An Introduction to Mössbauer Spectroscopy. (Plenum Press, New York, 1971).
10) V. I. Gol'danskii and R. H. Herber, Eds., Chemical Applications of Mössbauer Spectroscopy. (Academic Press, New York, 1968).
11) U. Gonser, Mat. Sci. Eng., 3 (1968) 1.
12) A. H. Muir Jr., K. J. Ando and M. H. Coogan, Mössbauer Effect Data Index, 1958-1965. (Interscience, New York, 1966).
13) J. G. Stevens and V. E. Stevens, Mössbauer Effect Data Index, 1969, (Plenum Press, New York, 1969).
14) J. G. Stevens and V. E. Stevens, Mössbauer Effect Data Index, 1972, (Plenum Press, New York, (1972).
15) I. J. Gruverman, Ed., Mössbauer Effect Methodology (Plenum Press, New York), Vols. 1–5, 1966–70.
16) A. J. Bearden, Ed., Third International Conference on the Mössbauer Effect, in Rev. Mod. Phys., 36 (1964) 333.
17) L. J. Swartzendruber, L. H. Bennett, E. A. Schoefer, W. T. Delong and H. C. Campbell, Welding J., 53 (1974) 1–S.
18) L. J. Swartzendruber and E. Siegel, Proc. of 19th Conf. on Magnetism and Materials, Boston, 1973.
19) H. Vollmar, Diplomarbeit im Universität des Saarlandes, 1973.
20) R. H. Nussbaum, D. G. Howard, W. L. Nee and C. F. Steen, Phys. Rev., 173 (1968) 653.
21) D. G. Howard and R. H. Nussbaum, Phys. Rev., B. 9 (1974) 794.
22) S. Nasu and Y. Murakami, Bull of Japan Inst. Met. (in Japanese), 11 (1972) 267.
23) L. R. Walker, G. K. Wertheim and V. Jaccarino, Phys. Rev. Letters, 6 (1961) 98.
24) B. D. Josephson, Phys. Rev. Letters, 4 (1960) 341.
25) S. Nasu and Y. Murakami, Phys. stat. sol., (b)46 (1971) 711.
26) B. Window, J. Phys. C, 3 (1970) S–323.
27) C. C. Tsuei, G. Longworth and S. C. H. Lin, Phys. Rev. 170 (1968) 603.
28) G. K. Wertheim, J. Appl. Phys., 32 (1961b) S–110.
29) A. J. F. Boyle and H. E. Hall, Rept. Progr. Phys., 25 (1962) 441.
30) H. L. Marcus, M. E. Fine and L. H. Schwartz, J. Appl. Phys., 38 (1967) 4750.
31) A. Nagarajan and P. A. Flinn, Appl. Phys. Letters, 11 (1967) 120.
32) A. Kelly and R. B. Nicholson, Progress in Material Science, Vol. 10, edited by B. Chalmers, 1963.
33) U. Gonser, Mössbauer Spectroscopy and its Applications, p. 89, Interscience Atomic Energy Agency, Vienna, 1972.
34) Y. Murakami, S. Nasu, S. Masuyama, A. Kawabe, T. Onishi and T. Kishimoto, Keikinzoku (in Japanese), 23 (1973) 492.
35) S. Nasu and U. Gonser, International Conference on Mössbauer Spectrometry, Bratislava, 1973.
36) M. Nishio, S. Nasu and Y. Murakami, Japan Inst. Met., (in Japanese), 34 (1971) 1173.
37) C. A. Stickels and H. R. Bush, Metal Trans., 2 (1971) 2031.
38) G. K. Wertheim and R. H. Herber, J. Chem. Phys., 38 (1963) 2106.